

A Comparison of the Laser Powder Interaction in Laser Powder Bed Fusion and Direct Energy Deposition Processes

*Original*

A Comparison of the Laser Powder Interaction in Laser Powder Bed Fusion and Direct Energy Deposition Processes / Aversa, A., Moshiri, M., Tusacciu, S., Busatto, M., Lai, M., Calignano, F., Manfredi, D.G., Pavese, M., Biamino, S., Lombardi, M.. - (2017). (Euro PM2017 Congress & Exhibition ).

*Availability:*

This version is available at: 11583/2703753 since: 2018-04-05T12:17:34Z

*Publisher:*

EPMA

*Published*

DOI:

*Terms of use:*

This article is made available under terms and conditions as specified in the corresponding bibliographic description in the repository

*Publisher copyright*

(Article begins on next page)



*Manuscript refereed by Prof Lars Nyborg (Chalmers University of Technology, Sweden)*

## **A Comparison of the Laser Powder Interaction in Laser Powder Bed Fusion and Direct Energy Deposition Processes**

Alberta Aversa<sup>1</sup> [alberta.aversa@polito.it](mailto:alberta.aversa@polito.it); Mandanà Moshiri<sup>1</sup> [mandana.moshiri@studenti.polito.it](mailto:mandana.moshiri@studenti.polito.it); Simona Tusacciu<sup>2</sup> [simona.tusacciu@irissrl.org](mailto:simona.tusacciu@irissrl.org); Mattia Busatto<sup>2</sup> [mattia.busatto@irissrl.org](mailto:mattia.busatto@irissrl.org); Manuel Lai<sup>2</sup> [manuel.lai@irissrl.org](mailto:manuel.lai@irissrl.org); Flavia Calignano<sup>3</sup> [flaviana.calignano@iit.it](mailto:flaviana.calignano@iit.it); Diego Manfredi<sup>3</sup> [diego.manfredi@iit.it](mailto:diego.manfredi@iit.it); Matteo Pavese<sup>1</sup> [matteo.pavese@polito.it](mailto:matteo.pavese@polito.it); Sara Biamino<sup>1</sup> [sara.biamino@polito.it](mailto:sara.biamino@polito.it); Mariangela Lombardi<sup>1</sup> [mariangela.lombardi@polito.it](mailto:mariangela.lombardi@polito.it)

<sup>1</sup>Politecnico di Torino, Corso Duca degli Abruzzi 24, Torino 10129, Italy

<sup>2</sup>IRIS S.r.l., Corso Unione Sovietica 612/21, Turin, TO, Italy

<sup>3</sup>CSFT@POLITO, Istituto Italiano di Tecnologia, Corso Trento 21, Torino 10129, Italy

© European Powder Metallurgy Association (EPMA). First published in the Euro PM2017 Congress Proceedings

### **Abstract**

Metal additive manufacturing (AM) is a class of innovative production technologies that allows the production of metal components layer by layer directly from a Computer Aided Design (CAD) model. The AM process of aluminium and aluminium alloys gained much interest in past years especially thanks to the high geometrical freedom, the peculiar microstructures and enhanced mechanical properties it is possible to achieve. However, the quality of final metal components strongly depends on the stability and the quality of each single scan track. Therefore, the understanding of the laser-powder interaction and of the phenomena that arise in the melt pool is a key aspect for the development of these technologies. In this work, AlSi10Mg single scan tracks (SSTs), produced by laser powder bed fusion (LPBF) and direct energy deposition (DED), were analysed and compared in order to select the most suitable range of parameters for each building process.

### **Introduction**

Among laser based metal additive manufacturing (AM) processes, direct energy deposition (DED) and laser powder bed fusion (LPBF) are the most relevant ones [1].

LPBF is a powder bed AM process in which a focused laser beam locally melts a thin layer of metal powder, according to the CAD data of the component [2]. The advantage of LPBF systems is mainly related to the geometrical accuracy and the possibility to build high resolution features.

The DED process, on the contrary, belongs to the blown powder AM class and uses a high power laser beam to create a melt pool; in the meantime powder is blown, by means of single or multiple nozzles, through the laser beam and into the melt pool [3]. DED technologies allow the production of large volume components and are characterised by high build up rates [4].

AlSi10Mg showed to be very suitable for AM processes thanks to its good fluidity in the molten state and to its composition close to the eutectic one. In past years, many studies were carried out on the microstructural and mechanical characterisation of LPBF AlSi10Mg parts [5–8]. On the contrary, to the best of our knowledge, only a few studies were carried out on the DED process of the Al-Si alloy [9,10]. In past years, some studies used single scan tracks (SSTs) analyses to have an insight of the most suitable building parameters for the LPBF of a specific alloy [11–13]. The main results of these analyses are the definition of process windows which highlight the most suitable power and scan speed for the AM process of a specific material and therefore the most suitable energy density (ED) [12]. SSTs experiments were carried out also for different purposes: Aboulkhair et al. for example used SSTs to investigate the microstructure and the nano-mechanical properties of LPBF AlSi10Mg [14]. Li et al. performed SSTs to investigate the processability of new materials by means of LPBF [15]. Furthermore, a few studies used this method to study the relevance and the effect of specific phenomena due to the laser powder bed interaction, such as the keyhole melting, the denudation, the balling and the spattering [16–18].

However, so far, any study has been carried out on DED single scan tracks and on the possibility to use these experiments as a preliminary analysis for the this process.

In the present work, AlSi10Mg SSTs, realized by LPBF and DED, were produced and compared in order to investigate the possibility to use this method as a guideline for the selection of the most suitable building parameters and for understanding the phenomena that arise during the laser scanning in blown powder AM processes.

**Materials and methods**

For the LPBF process a gas atomised AlSi10Mg powder provided by EOS GmbH was used while for the DED process the AlSi10Mg gas atomised powder was provided by LPW Technology Ltd. From FESEM micrographs of these powders, shown in Fig. 1, it can be noticed that both have a roughly spherical shape and contain some satellites. As expected, DED particles are characterised by larger size than the LPBF ones.

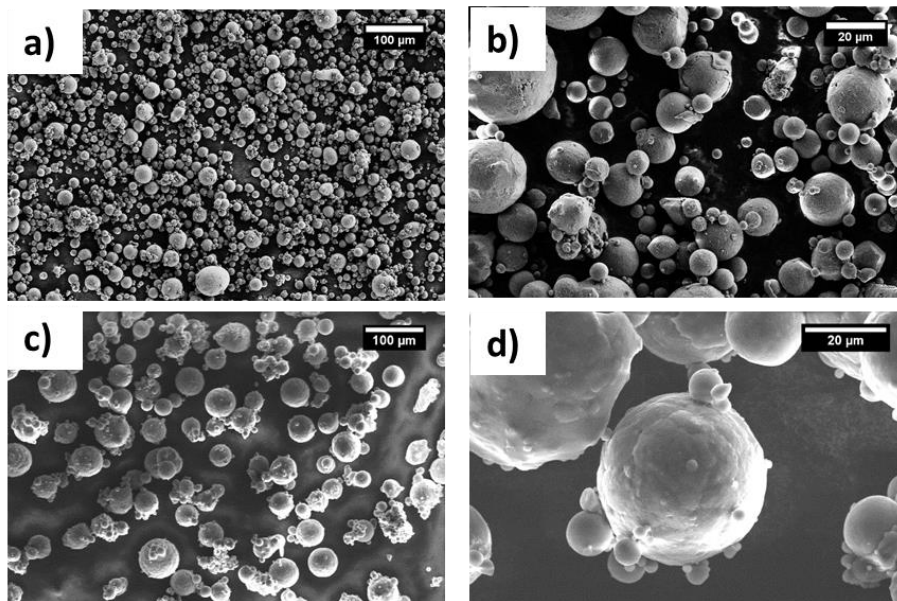


*Fig. 1 FESEM micrographs of AlSi10Mg particles used for a) and b) LPBF and c) and d) DED processes.*

The LPBF equipment used in this project is an EOS M270 Dual Mode system which uses a focused Yb laser beam ( $\lambda=1064$  nm) and works in protective argon atmosphere (Fig. 2 a)). For this process the laser power (P) and the scanning speed (v) were varied in the following ranges: P= 50 – 195 W and v = 50 – 3000 mm/s.

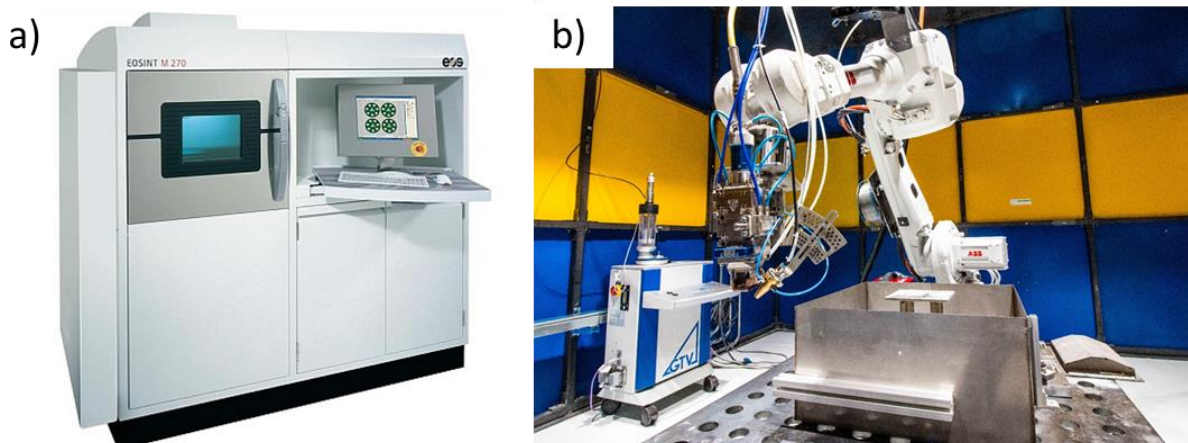


*Fig. 2 Images of a) the EOS LPBF and b) the DED systems.*

The DED system is constituted by an experimental cell with dimensions 4,7 x 5,9 x 3,6 m, equipped with an ABB anthropomorphic robot arm (Fig. 2 b)). This system uses a 3 kW IPG fibre laser to melt metal powders blown by means of GTV powder feeder through a lateral nozzle which anticipate the laser path. An inert shielding gas protect the melt pool from oxidation. The main parameters varied in these experiments were the focus position (from – 3 mm to + 3 mm), that indicates the focus location with respect to the building platform, and the power amount (indicated as %). The scan speed and the powder flow rate were kept constant and 60 mm/s and 0.67 g/s, respectively.

All SSTs were characterised on-top by means of a stereomicroscope Leica EZ4 and in cross-section by means of an optical microscope (OM) Leica DMI 5000 M and by means of a Field Emission Scanning Electron Microscope (FESEM) SEM-FEG Assing SUPRA 25, Zeiss. The Image J software was used for the characterisation of the single scan geometry.

### **Results and discussion**

For the LPBF process, the on-top analyses allowed the identification of five stability conditions, reported in Fig. 3. With low energy density any SST was formed (Fig. 3 a)); when slightly higher energy densities were used, “balling” arised because of the effect of the surface tension that breaks the scan in separated balls (Fig. 3 b)). “Thin and stable” scans were formed when an intermediate ED value was used (Fig. 3 c)), whereas higher energy densities caused the formation of “irregular” and “too thick lines” (Fig. 3 d) and e)).

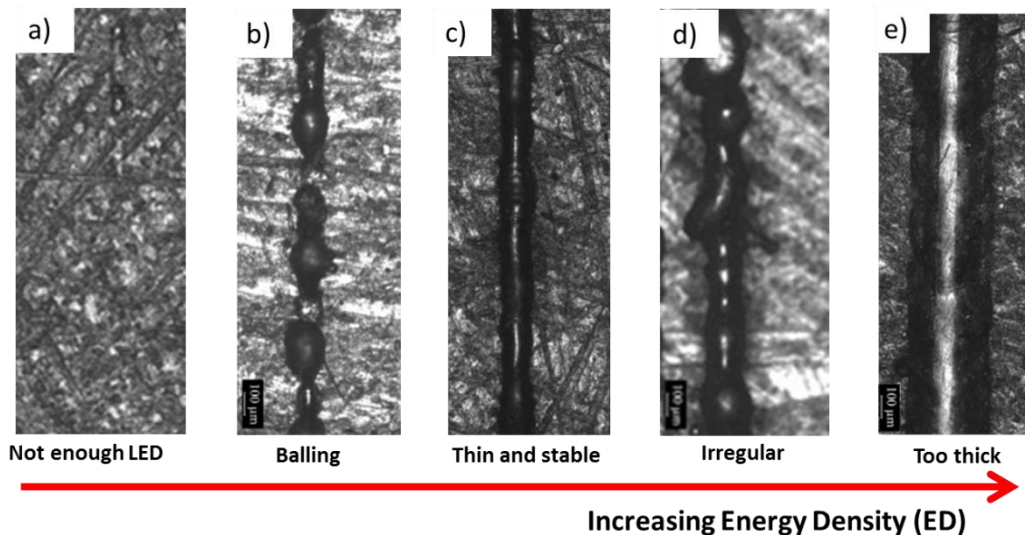


*Fig. 3 On-top optical micrographs of different LPBF SSTs morphologies.*

Based on these stability conditions it is possible to define a process window that indicates the morphology of the AlSi10Mg SSTs obtained with each set of parameters (Fig. 4).

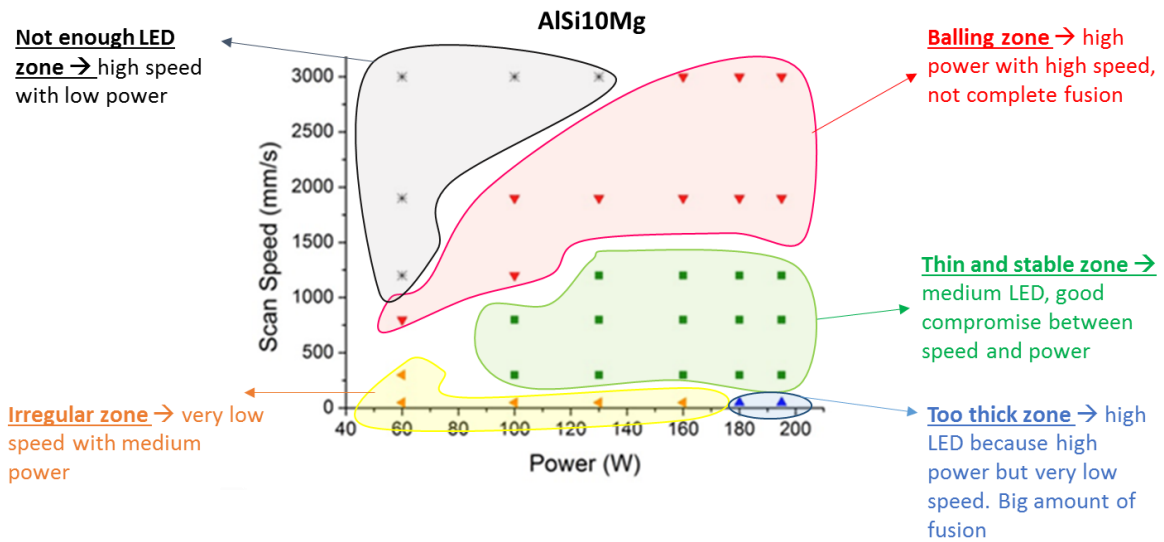


Fig. 4 LPBF process window for AlSi10Mg SSTs.

On-top optical micrographs of DED SSTs, shown in Fig. 5, revealed that, in this case, only two morphologies were observed.

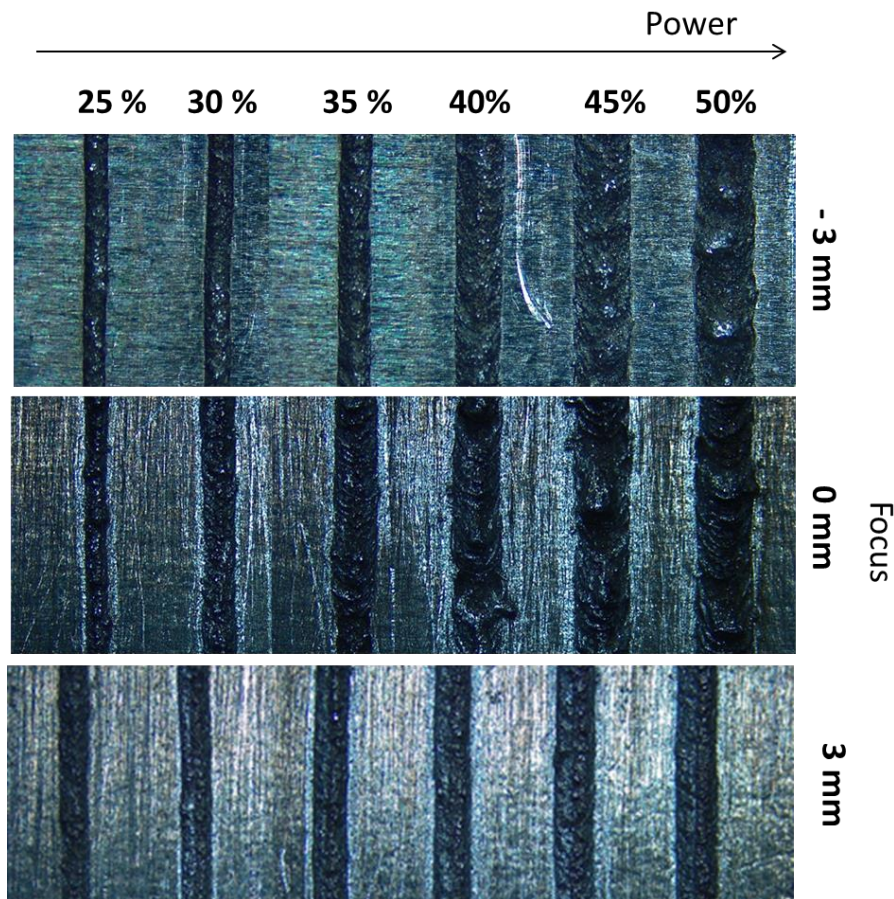
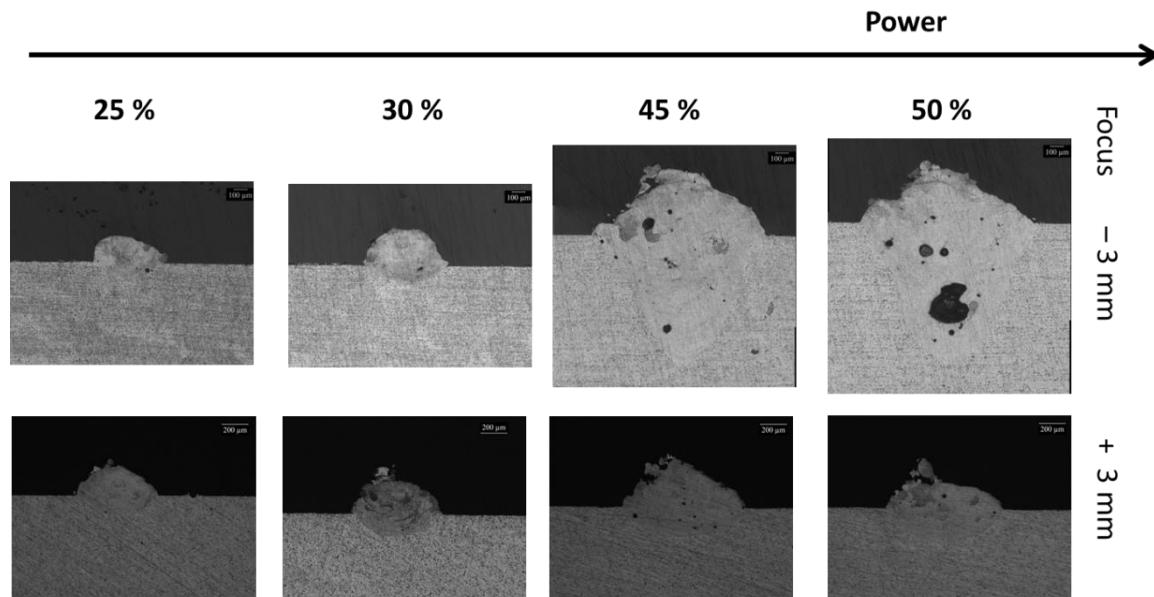


Fig. 5 On-top micrographs of DED SSTs built with  $v = 60 \text{ mm/s}$ .

The comparison of on-top micrographs suggests that the focus position has a strong effect on the stability of the melt pool. This might be related to size of the beam in the area in which the powder flow crosses it. When the focus is inside the material ( $f = -3 \text{ mm}$ ) most of the powder melts in flight because of the large laser beam in the intersection area. On the contrary, when SSTs are built with a focus outside from the material, only some particles cross the laser beam and melt.

Also in this case, as in the LPBF process, high energy density values caused irregularities on the melt pool. However, in the DED process any stable “too thick lines” were observed. The lack of stable too thick lines could be related to the shielding and the carrier gases, that caused the waviness scan track. Furthermore, for the blown powder system, “balling” was not observed probably because the different process allows to maintain the continuity of the melt pool.

From the comparison of the cross section micrographs it can be also noted that relatively low power allowed the obtainment of dense and regular tracks (Fig. 6). In fact, when high power values were used, deep and irregular scans were formed because of a keyhole melting phenomenon. SSTs in which a keyhole melting arised were also characterised by the presence of some pores in the lower area (Fig. 6). Furthermore, it is possible to measure the melt pool dimensions through image analysis of cross section micrographs to select the most suitable X and Z displacement for the obtainment of a suitable overlapping and therefore dense samples. For instance, the scan built with the lower power and with positive focus had a width and a total height of about 500 and 400  $\mu\text{m}$ , respectively.



*Fig. 6 Cross-section micrographs of some DED SSTs.*

## **Conclusions**

In this study AISi10Mg SSTs made by two metal AM processes were characterised and compared. The main results can be summarised as follows:

- LPBF SSTs can be easily classified by means of on-top micrographs and process windows that indicate that five stability zones can be obtained varying the process parameters;
- In the DED process more factors participate to the scan consolidation and therefore a different process window is observed;
- SSTs studies seem to be a promising way for preliminary studies of new materials for both AM technologies.

## **Acknowledgements**

The authors would like to acknowledge the European research project belonging to Horizon 2020 Borealis, the 3A energy class Flexible Machine for the new Additive and Subtractive Manufacturing on next generation of complex 3D metal parts and the European research project belonging to the VII framework program AMAZE, Additive Manufacturing Aiming Toward Zero Waste and Efficient Production of High-Tech Metal Products.

## **Funding**

This project has received funding from European Union’s Horizon 2020 research and innovation programme under grant agreement No 636992.

**References**

- [1] A. Gasser, Comparison of Additive Manufacturing Technologies SLM and LMD, (2014) 69572.
- [2] W.E. Frazier, Metal additive manufacturing: A review, *J. Mater. Eng. Perform.* 23 (2014) 1917–1928. doi:10.1007/s11665-014-0958-z.
- [3] N. Shamsaei, A. Yadollahi, L. Bian, S.M. Thompson, An overview of Direct Laser Deposition for additive manufacturing; Part II: Mechanical behavior, process parameter optimization and control, *Addit. Manuf.* 8 (2015) 12–35. doi:10.1016/j.addma.2015.07.002.
- [4] G. Marchese, X. Garmendia Colera, F. Calignano, M. Lorusso, S. Biamino, P. Minetola, D. Manfredi, Characterization and Comparison of Inconel 625 Processed by Selective Laser Melting and Laser Metal Deposition, *Adv. Eng. Mater.* (2016) 1–9. doi:10.1002/adem.201600635.
- [5] N. Read, W. Wang, K. Essa, M.M. Attallah, Selective laser melting of AlSi10Mg alloy: Process optimisation and mechanical properties development, *Mater. Des.* 65 (2015) 417–424. doi:10.1016/j.matdes.2014.09.044.
- [6] J. Wu, X.Q. Wang, W. Wang, M.M. Attallah, M.H. Loretto, Microstructure and strength of selectively laser melted AlSi10Mg, *Acta Mater.* 117 (2016) 311–320. doi:10.1016/j.actamat.2016.07.012.
- [7] F. Trevisan, F. Calignano, M. Lorusso, J. Pakkanen, A. Aversa, E. Ambrosio, M. Lombardi, P. Fino, D. Manfredi, On the Selective Laser Melting (SLM) of the AlSi10Mg Alloy: Process, Microstructure, and Mechanical Properties, *Materials (Basel)*. 10 (2017) 76. doi:10.3390/ma10010076.
- [8] M. Lorusso, A. Aversa, D. Manfredi, F. Calignano, E.P. Ambrosio, D. Ugues, M. Pavese, Tribological Behavior of Aluminum Alloy AlSi10Mg-TiB<sub>2</sub> Composites Produced by Direct Metal Laser Sintering (DMLS), *J. Mater. Eng. Perform.* 25 (2016) 1–9. doi:10.1007/s11665-016-2190-5.
- [9] Y.T. J, M Javidani J Arreguin-Zavala, J. Danovitch, Brochu, Additive Manufacturing of AlSi10Mg Alloy Using Direct Energy Deposition: Microstructure and Hardness Characterization, *J. Therm. Spray Technol.* 26 (2017) 587–597. doi:10.1007/s11666-016-0495-4.
- [10] G.P. Dinda, A.K. Dasgupta, J. Mazumder, Surface & Coatings Technology Evolution of microstructure in laser deposited Al – 11 . 28 % Si alloy, *Surf. Coat. Technol.* 206 (2012) 2152–2160. doi:10.1016/j.surfcoat.2011.09.051.
- [11] J.P. Kruth, L. Froyen, J. Van Vaerenbergh, P. Mercelis, M. Rombouts, B. Lauwers, Selective laser melting of iron-based powder, *J. Mater. Process. Technol.* 149 (2004) 616–622. doi:10.1016/j.jmatprotec.2003.11.051.
- [12] T.H.C. Childs, C. Hauser, M. Badrossamay, Mapping and Modelling Single Scan Track Formation in Direct Metal Selective Laser Melting, *CIRP Ann. - Manuf. Technol.* 53 (2004) 191–194. doi:10.1016/S0007-8506(07)60676-3.
- [13] E. Librera, A. Science, P. Torino, C. Duca, Study of Single Tracks with AlSi10Mg and Composites Powders, (n.d.).
- [14] N.T. Aboulkhair, I. Maskery, C. Tuck, I. Ashcroft, N.M. Everitt, On the formation of AlSi10Mg single tracks and layers in selective laser melting: Microstructure and nano-mechanical

- properties, *J. Mater. Process. Technol.* 230 (2016) 88–98. doi:10.1016/j.jmatprotec.2015.11.016.
- [15] X.P. Li, C.W. Kang, H. Huang, L.C. Zhang, T.B. Sercombe, Selective laser melting of an Al86Ni6Y4.5Co2La1.5 metallic glass: Processing, microstructure evolution and mechanical properties, *Mater. Sci. Eng. A.* 606 (2014) 370–379. doi:10.1016/j.msea.2014.03.097.
- [16] W.E. King, H.D. Barth, V.M. Castillo, G.F. Gallegos, J.W. Gibbs, D.E. Hahn, C. Kamath, A.M. Rubenchik, Observation of keyhole-mode laser melting in laser powder-bed fusion additive manufacturing, *J. Mater. Process. Technol.* 214 (2014) 2915–2925. doi:10.1016/j.jmatprotec.2014.06.005.
- [17] M.J. Matthews, G. Guss, S. a. Khairallah, A.M. Rubenchik, P.J. Depond, W.E. King, Denudation of metal powder layers in laser powder bed fusion processes, *Acta Mater.* 114 (2016) 33–42. doi:10.1016/j.actamat.2016.05.017.
- [18] D. Gu, Y. Shen, Balling phenomena during direct laser sintering of multi-component Cu-based metal powder, *J. Alloys Compd.* 432 (2007) 163–166. doi:10.1016/j.jallcom.2006.06.011.